MADRID
inter.noise 2019
June 16 - 19
NOISE CONTROL FOR A BETTER ENVIRONMENT

# Atmospheric propagation of aircraft acoustic signature from high altitude

**Sebastian Ghinet**[1]
**Andrew Price**[2]
**Gilles A. Daigle**[3]
**Michael R. Stinson**[4]
**Anant Grewal**[5]
**Viresh Wickramasinghe**[6]

**NRC Aerospace Research Centre, Flight Research Laboratory**
**1200 Montreal Road**
**Ottawa, Ontario, K1A 0R6, Canada**

## ABSTRACT

**A large number of computational approaches for acoustic atmospheric propagation have been developed and extensively validated during the past decades. Generally, the model of choice to predict outdoor sound propagation is the Parabolic Equation (PE) because it can simultaneously account for all the factors that can affect the propagation. These factors include geometrical spreading, atmospheric absorption, ground effects, refraction and turbulence. However, in the case of a high-altitude aircraft flying overhead, a microphone near the ground would be located outside the solid angle of validity of the PE. In this paper an impedance plane formulation that does not account for refraction and a Fast Field Program (FFP) that does not account for turbulence were implemented to predict the acoustic spectra of an aircraft propagating through the atmosphere at various altitudes, distances and angles. The paper aims at presenting the two theoretical approaches, the numerical and testing validation results and discussing the influence of various factors on the aircraft sound propagation from high altitude. In particular it will be shown that refraction is negligible, but that meteorological measurements made only at ground level are insufficient to estimate the atmospheric absorption.**

**Keywords:** Aircraft Noise, Acoustic Waves, Atmospheric Sound Propagation
**I-INCE Classification of Subject Number:** 24

---

[1] Sebastian.Ghinet@nrc-cnrc.gc.ca
[2] Andrew.Price@nrc-cnrc.gc.ca
[3] Gilles.Daigle@nrc-cnrc.gc.ca
[4] Michael.Stinson@nrc-cnrc.gc.ca
[5] Anant.Grewal@nrc-cnrc.gc.ca
[6] Viresh.Wickramasinghe@nrc-cnrc.gc.ca

## 1. INTRODUCTION

The accurate prediction of outdoor acoustic propagation and sound transmission loss from a source to a receiver is influenced by multiple acoustic and meteorological factors such as the geometrical spreading, atmospheric absorption, ground impedance, ground topography, refraction due to wind and temperature profiles above the ground, and atmospheric turbulence. A review of these factors can be found in [1]. Over the past few decades, a number of different models have been developed to predict the outdoor sound propagation. Most models account for some of the factors listed above, but not all. A limited number of models attempt to account for all the factors simultaneously, but these models are complex and time consuming to use. The most common models in use today include the impedance plane formulation, hybrid ray-based models, the Fast Field Program (FFP), and the Parabolic Equation (PE). A good summary of these models can be found in [2]. In particular, this reference defines benchmark cases by which the models have been validated against each other. A detailed discussion of these models can be found in [3].

The paper aims at addressing the numerical simulation and test validation of aircraft noise propagation and transmission loss through atmosphere from cruise altitude to the ground. In the case of a high-altitude aircraft, it is anticipated that refraction will be negligible while geometrical spreading, atmospheric absorption, ground effects, and turbulence would be the main factors affecting the propagation. Therefore, the impedance plane formulation was considered here since it takes into account all these factors. In order to quantify the effects of refraction the FFP approach was also considered. However, the FFP is a numerical solution that could be very time consuming depending on frequency and range and it does not capture the effects of atmospheric turbulence.

The implemented numerical approaches were validated using fly-by aircraft acoustic data. The National Research Council’s Flight Research Laboratory Convair 580 aircraft was flown at four altitudes (1000 ft, 2000 ft, 8000 ft and 12000 ft) at the Smiths Falls Montague Airport, located in Ontario, Canada. Low-altitude propagated acoustic data measured at ground-level was used to characterize the aircraft’s acoustic signature. Subsequently, high-altitude propagated acoustic data at a ground height of 1.5 m was predicted using the acoustic propagation models. The predictions were validated using measured data from flight tests.

## 2. ATMOSPHERIC PROPAGATION NUMERICAL APPROACHES

The factors that are most likely to affect the sound propagation from a high altitude flying aircraft to a receiver near the ground are briefly presented.

The phenomenon of *geometrical spherical spreading* of a sound wave implies that the sound level decreases at a rate of 6 dB per doubling of distance and is not a function of frequency in the absence of atmospheric absorption.

The *absorption of acoustic energy by the atmosphere* occurs through viscous effects, heat conduction and absorption by molecular relaxation. The compressional energy of the acoustic wave is redistributed into rotational and vibrational modes through collisions of the molecules. As a consequence, in contrast to geometrical spreading, the absorption of sound energy by the atmosphere is a function of frequency, temperature, humidity, and pressure. The atmospheric absorption is weak at low frequencies, but increases rapidly as the frequency increases [1]. The consequence for an aircraft flying at an elevated altitude is that the lower frequencies will propagate to the ground while the higher frequencies will be greatly attenuated. Further, since temperature, humidity and pressure vary strongly with height above the ground, it was necessary to integrate the absorption along the propagation path between the aircraft and receiver above the ground using the temperature, humidity, and pressure profiles.

The *ground effect* on the sound received at an offset height from the ground is characterized by the interference between the direct and the reflected fields as well as by the ground surface porosity. The more important effect is the phase change of the reflected field upon reflection as function of ground porosity and the grazing angle [1]. For example, a very small grazing angle will result in a phase change close to 180°. The interference between the direct field and the reflected field could be constructive or destructive depending on the difference in the path length. For a constructive interference between the direct and reflected fields, the addition of the two increases the sound pressure levels by 6 dB while dips occur at frequencies where there is cancellation between the two fields (destructive interference). The position of the dips is expected to change as the porosity of the ground changes.

The sound wave propagation paths from a point source *S* to a receiver *R* positioned above a ground plane at heights $h_s$ and $h_r$ respectively, at a propagation range *d* and a grazing angle $\varphi$ are shown in Figure 1. The path lengths of the direct and reflected sound waves are $r_d$ and $r_r$ respectively.

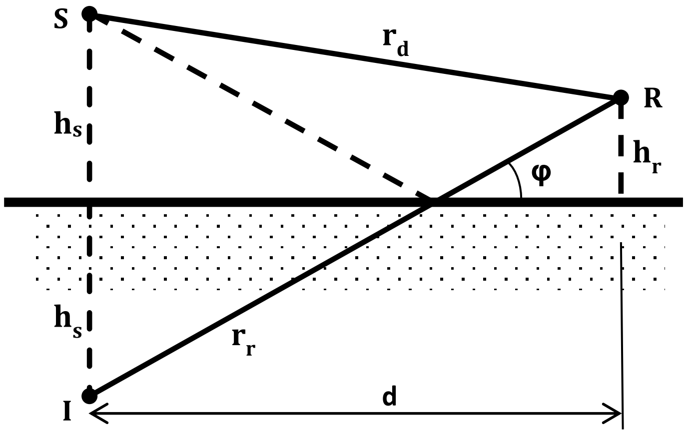


*Figure 1. Sound propagation paths from source S to receiver R above a reflective ground plane.*

The *refraction of sound* is attributed to the change in the speed of sound as function of the temperature and wind speed above the ground resulting in a change of the grazing angle and ultimately in a shift of the interference dips position [1]. However, in the case of a high-altitude aircraft flying overhead, the propagation is in the vertical direction through the wind and temperature profiles and the shift in grazing angle is anticipated to be negligible.

Atmospheric random variations in temperature, wind speed, pressure, and density affect acoustic wave propagation. However, in practice only the temperature and wind speed variations play a significant role [4, 5]. These random variations, or *turbulence,* affect the integrity of the acoustic wave fronts resulting in fluctuations in phase and amplitude, with increasing propagation distance. In the case of an elevated source, one main effect of turbulence is to reduce the depth of the dips in the spectrum, resulting from the ground effect destructive interference.

### 2.1 Impedance plane formulation

All acoustic data was measured within the airport perimeter. The airport ground was flat and mainly covered with grass in the areas surrounding the sound measuring stations.

A reference acoustic pressure spectrum of the NRC Convair 580 aircraft was measured at low altitude, and after correcting for geometric spreading and atmospheric absorption to estimate an equivalent point source model, was used as an input to the propagation models in order to generate predicted spectra at higher altitudes and larger distances. Reference acoustic pressure spectra were measured during flight at the lowest permissible altitude of 1000 ft and, in addition, at 2000 ft.

In order to eliminate ground effects (peaks and dips due to constructive or destructive interference between the direct and reflected fields respectively) as well as the effects of the finite ground porosity, the measurements were made using microphones mounted directly ($h_r$ < 0.01m) on a 4 ft x 4 ft x 1 in sheet of plywood.

The reference spectra ($PSD_{Ref}$) were corrected for geometrical spreading or Inverse Square Law ($A_{Div}$) and atmospheric absorption ($A_{atm}$) in order to calculate the equivalent point source PSD of the aircraft ($PSD_{EqS}$) using the following relation:

$$PSD_{EqS} = PSD_{Ref} - A_{Div}(r_d) + A_{atm}(r_d) - A_{ground} \text{, (dB);} \tag{1}$$

with, $$A_{Div} = 20\log_{10}\left(\frac{1}{r_d}\right) \text{, (dB);} \tag{2}$$

and $r_d$ is the path distance between the source and receiver, $A_{ground}$ = 6dB to account for the fact that the microphone was mounted directly on a reflective ground. At lower frequencies and shorter distance, the correction for the atmospheric absorption becomes negligible. The atmospheric absorption of sound ($A_{atm}$) was calculated using the approach presented in Ref. [8].

The equivalent free field point source PSD was subsequently used in the model to predict the higher altitude PSD spectra propagated through the atmosphere to the receiver ($PSD_{HAlt}$) using the following relation:

$$PSD_{HAlt} = PSD_{EqS} + TL\text{;} \tag{3}$$

where, $TL$ is the total sound attenuation or Transmission Loss defined as the sum of three main attenuation terms as follows:

$$TL = A_{Div} + A_{atm} + A_{misc}\text{;} \tag{4}$$

where, $A_{div}$ is the attenuation due to spherical spreading as defined in (2), $A_{atm}$ is the attenuation due to atmospheric absorption [8], and $A_{misc}$ is the attenuation due to all other physical phenomena (atmospheric turbulence, ground absorption, etc.).

The ground surface characteristic impedance $Z_c$ and the acoustic propagation constant $k_b$ were calculated using the empirical model approach developed by Delany and Bazley [9]:

$$Z_c = \rho_0 c_0\left(1 + 9.08\left(\frac{\sigma}{f}\right)^{0.75} + i11.9\left(\frac{\sigma}{f}\right)^{0.73}\right)\text{;} \tag{5}$$

$$k_b = \frac{\omega}{c_0}\left(1 + 10.8\left(\frac{\sigma}{f}\right)^{0.7} + i10.3\left(\frac{\sigma}{f}\right)^{0.59}\right)\text{;} \tag{6}$$

with $0.01 < \dfrac{\sigma}{f} < 1$;

where, $\rho_0$ and $c_0$ are the density of the air and the speed of sound in air, and $\omega = 2\pi f$ is the angular frequency and $\sigma$ is the static airflow resistivity. In the implemented model the flow resistivity was actually, as assumed by Delany and Bazley [1, 10], an effective flow resistivity accounting for the ground porosity. The value for the effective flow resistivity utilized in the model for the grass field was 300 cgs.

In order to account for turbulence effects on sound propagation above a ground plane of complex impedance for an assumed spherically symmetric source, the mean-square received pressure was calculated using the following expression [11]:

$$\left\langle \overline{p^2} \right\rangle = \frac{1}{r_d^2} + \frac{|Q|^2}{r_r^2} + \frac{2|Q|}{r_r r_d}\cos\left[k\left(r_r - r_d\right) + \theta\right]\gamma \; ; \tag{8}$$

where, $Q$ is a function of $r_r$, $Z_s$, $k$, $\varphi$ and is the complex spherical wave reflection factor and was calculated using the approach presented in Ref. [12], The variable $\gamma$ accounts for atmospheric turbulence and is given by:

$$\gamma = \exp\left(-\left(\frac{\sqrt{\pi}}{2}\right)\left\langle \mu^2 \right\rangle k^2 r_d L\left(1 - \frac{\sqrt{\pi}}{2}\frac{erf\left(\frac{h}{L}\right)}{\frac{h}{L}}\right)\right) \; ; \tag{9}$$

with, $erf$ the error function, $L$ the Gaussian turbulence scale, $\left\langle \mu^2 \right\rangle$ is the variance of the index of refraction and $k$ is the acoustic wavenumber ($k=2\pi f/c_0$). The effective strength of the atmospheric turbulence was estimated empirically [5] according to the wind speed ($Ws$) as follows:

1. Very low turbulence strength for $Ws < 1$ m/s; $\left\langle \mu^2 \right\rangle$=0.5e$^{-6}$;
2. Low turbulence strength for 1 m/s $\leq Ws <$ 3 m/s; $\left\langle \mu^2 \right\rangle$ =2e$^{-6}$;
3. Moderate turbulence strength for 3 m/s $\leq Ws <$ 6 m/s; $\left\langle \mu^2 \right\rangle$ =10e$^{-6}$;
4. Strong turbulence strength for 6 m/s $\leq Ws \leq$ 10 m/s; $\left\langle \mu^2 \right\rangle$ =15e$^{-6}$;
5. Very strong turbulence strength for $Ws >$ 10 m/s; $\left\langle \mu^2 \right\rangle$ =25e$^{-6}$.

The attenuation term due to the ground and turbulence effects was calculated as follows:

$$A_{Div} + A_{misc} = 10log_{10}\left(\left\langle \overline{p^2} \right\rangle\right) \; . \tag{10}$$

The Transmission Loss is then obtained by adding the attenuation due to atmospheric absorption.

Impedance plane formulation was compared with FFP approach results and measured data to demonstrate the validity of the implemented approach and observe the influence of the various parameters on the received acoustic spectra from high altitude flying-by aircraft. The FFP implementation followed the theoretical approach described in Ref. [1, 2].

## 3. MEASUREMENT PROCEDURE AND DATA ANALYSIS

Significant consideration was put into the development of the experimental flight test plan to record the Convair aircraft acoustic pressure spectra.

Five acoustic measurement stations were deployed at the Smiths Falls Montague aerodrome for the purposes of data redundancy and the capability to capture different aircraft noise emission angles; the locations are depicted in Figure 2. As presented in Ref. [6, 7], portable GPS dongles were attached to each measurement station to allow for time synchronization of the five microphone channels with the aircraft flight data system. This allowed for accurate knowledge of aircraft altitude, range, velocity and emission angle.

Measurements of the environmental conditions; air temperature, wind speed, wind direction and air relative humidity were required to validate the acoustic propagation models. The environmental data as function of altitude, the aircraft spatial positioning data and the acoustic pressure data were all required to be time-synchronized. Additionally, certain experimental considerations had to be accounted for, specifically the non-instantaneous propagation of the sound spectra from the aircraft to the ground and the tracking of the aircraft noise emission angle. For the purposes of validation and calibration, it was vital to capture comparable noise emission angles at the high-altitude and the low-altitude fly-bys [7].

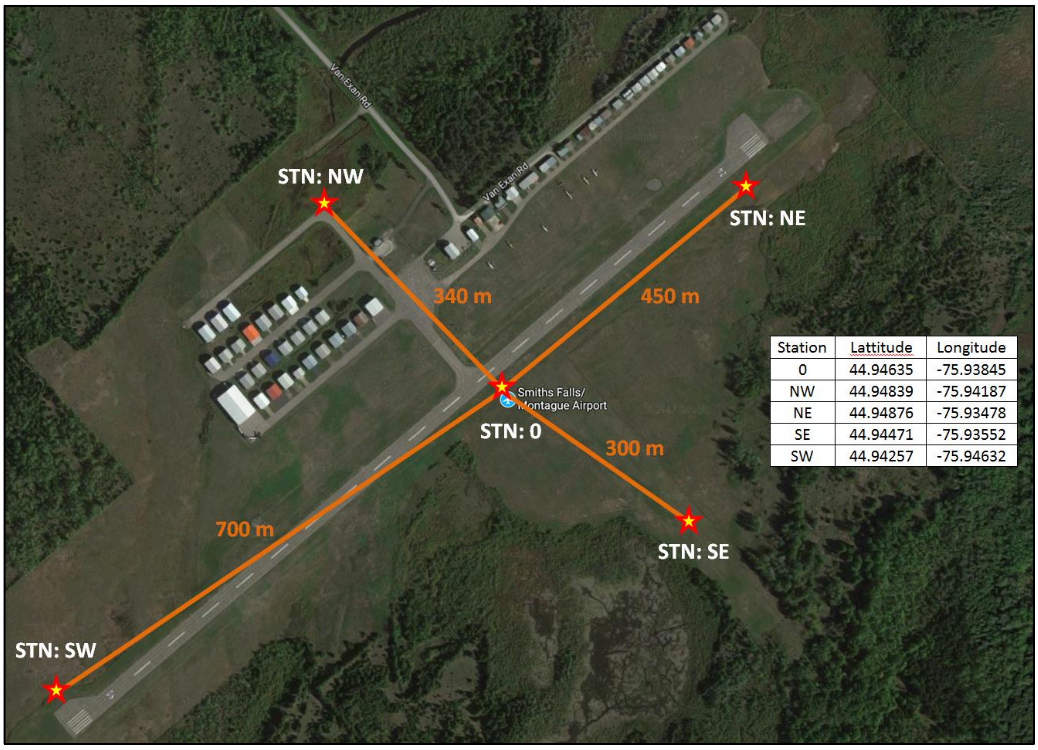

*Figure 2: Smiths Falls Montague Airport Acoustic Measurement Locations*

The atmospheric parameters were measured utilizing sensors mounted onboard the Convair aircraft. Further, the Convair flew at 1000 ft, 2000 ft, 8000 ft and 12000 ft. Thus the atmospheric parameters data was recorded as the aircraft ascended to the higher altitudes. This data was merged to values measured on the ground. It was necessary to take into account the variations of air temperature, RH, and atmospheric pressure as a function of height since they vary strongly with height. The FFP calculations required the wind and temperature profile as a function of height. A wind sensor was used to measure wind speed and direction. Cloud cover was used to estimate the thermal stability of the atmosphere. The wind and temperature profiles were then generated using similarity scaling equations [3]. Since these equations are only valid up to a few hundred meters, the profiles were estimated to the higher altitude profiles generated by a model developed by the National Oceanic and Atmospheric Administration (NOAA) in the United States [13]. The NOAA model uses data generated by local Environment Canada weather stations.

The flight testing procedure, the instrumentation and data analysis were extensively presented in Ref. [6, 7]. Moreover critical considerations accounted for in this study, such as Doppler shift effect, noise emission direction and propagation time delay, were presented in Ref. [7].

The data analysis conducted for this task had to take into consideration some specific characteristics of the acquired time signal and the dynamics of the problem under study. Considering that the Convair acoustic pressure amplitude at low altitude could change rapidly when flying overhead at approximately 100 $m/s$ speed, sufficiently small time windows were required in order to capture signals representative of different portions of the flight. It was determined that 1-second samples of data were the optimal compromise as samples shorter than this exhibited high sample-to-sample variability. Moreover, for a 1-second sample at a sampling rate of 25,600 Hz it was found that a selection of a Segment Length $N_{SL}$ = 8192 was optimal for the Convair acoustic data.

Background noise levels for the Smiths Falls Montague aerodrome site on the day of measurement were measured when the Convair aircraft was not present. A first set of data was recorded for the half hour before the Convair approached the Smiths Falls site. Consecutive 1-second snippets of data were considered and the power spectrum of each was calculated. The spectra are shown in Figure 3. A large variability has been observed between spectra, with an overall sound pressure level range between 40 and 60 dB.

For each spectrum, the equivalent sound pressure level was calculated and plotted as a function of time to show the variability of the overall background sound pressure level; this is shown in Figure 4. It can be observed in Figure 4 that the background noise level changed significantly, ranging between 50 dB and 100 dB over the course of the half-hour period considered in this case. Several large spikes of noise activity can be observed at different points in this plot: these correspond to a club aircraft performing “touch-and-go” manoeuvres. In between these spikes, there was other activity, including road traffic noise, air traffic noise and conversations between project personnel. Given the large variability in the different data sets of ambient noise, it was appropriate to treat the data statistically. In doing so, loud irregular events (such as the touch-and-goes) were avoided and the stationary background contributions were retained primarily: hence, only spectra with Leq below 70 dB were used.

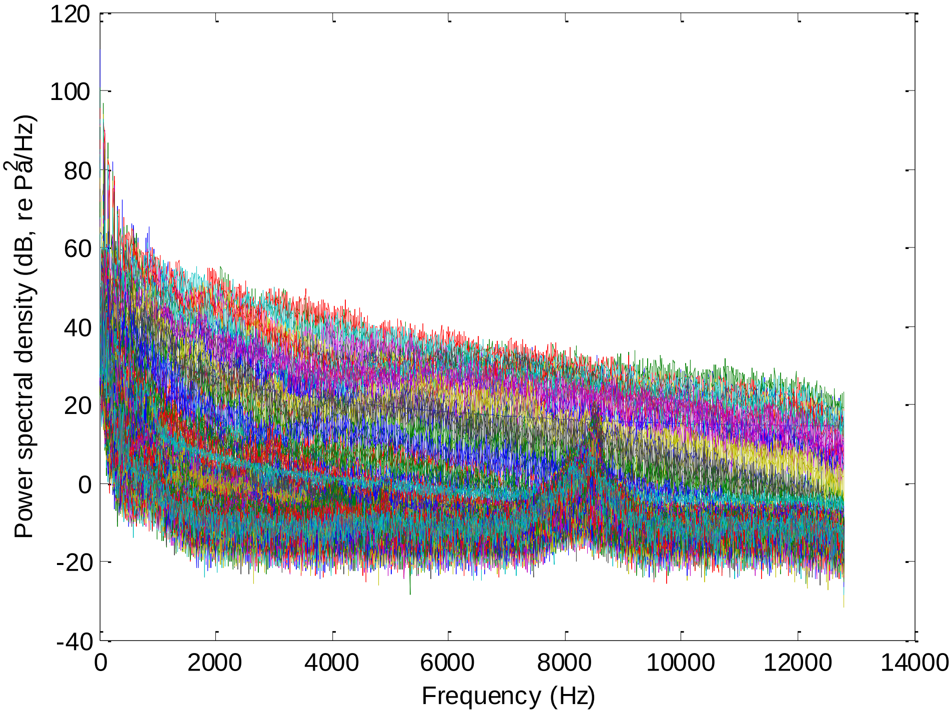


*Figure 3. Power Spectral Density Plots of the Smiths Falls Background Noise.*

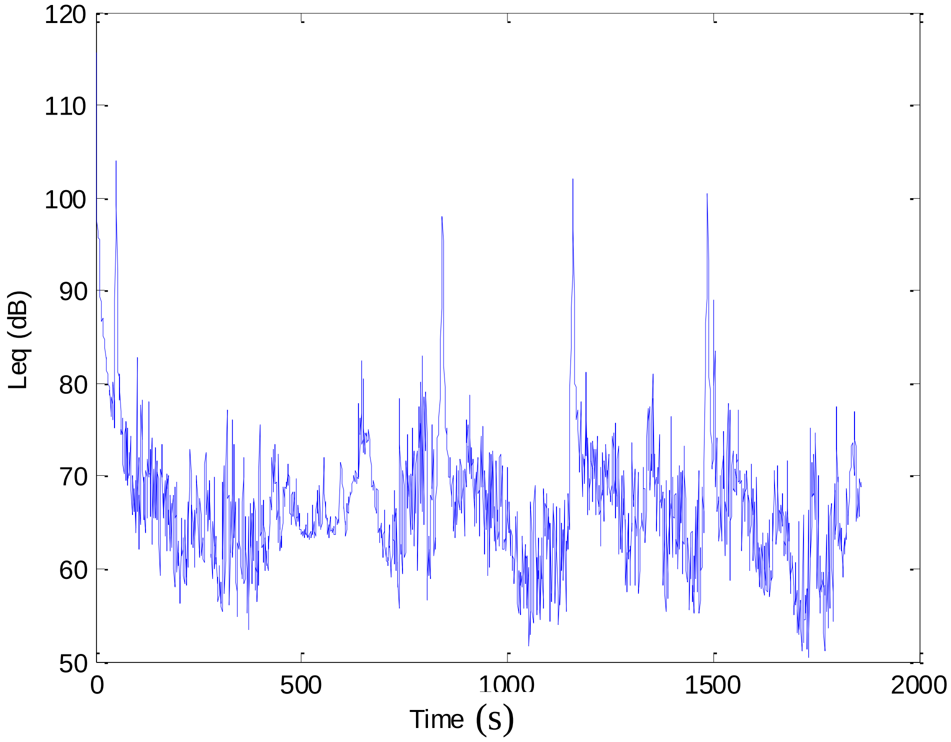

*Figure 4. Background Noise Overall Sound Pressure Level Variation with Time.*

## 3.2 Model propagation validation

The main objective of the study was the validation of the testing procedure (using low-altitude reference spectra to predict the high-altitude spectra) and to demonstrate that the models have the ability to adequately account for the environmental behaviour to predict sound propagation from a high-altitude flying aircraft. Consequently the selection of the flight segments for both the reference low-altitude spectra and high-altitude spectra was oriented toward segments where the ambient background noise was observed to be the lowest.

In order to determine the importance of using amplitude dependent measured meteorological data versus at ground level, the impedance plane approach was used to calculate the sound atmospheric propagation transmission loss for both cases. The results are shown in Figure 5. It can be observed that meteorological measurements made only at ground level are insufficient to accurately estimate the atmospheric absorption.

The predicted and the measured aircraft spectra at 8000 ft and 12000 ft are shown in Figure 6 to Figure 9. The red curve represents the measured spectrum while the spectrum predicted by the impedance plane formulation using the low-altitude signature as the reference is represented by the black curve. The open circles represent the predictions of the FFP model at each 3rd octave frequency. The blue curve represents the median ambient background noise measured during the duration of the trials. This curve was obtained by calculating the background noise spectra at sample intervals throughout the day and selecting the median overall sound pressure level's corresponding spectra.

It can be observed that for an altitude of 8000 ft the frequencies of the two measured and predicted harmonic peaks (around 70 and 140 Hz) are well captured by the Impedance Plane approach (Figure 6 and Figure 7). While the two harmonic peaks are well predicted at 2.08km range case (Figure 6) it can be observed a negligible shift in the prediction for 4.38 km range (Figure 7). This phenomenon is expected due to the Doppler shift when using sound samples with a slight mismatch between the azimuthal angle and the angle of elevation of the reference low-altitude segment of the flight and the high-altitude segment [7].

The predicted and the measured aircraft spectra at 12000 ft are shown in Figure 8 and Figure 9. It can be observed that the measured and predicted levels are generally in good agreement. There is a good match between the frequencies of the two harmonic peaks, but the measured level of second harmonic, in Figure 9, is greater that the predicted level due to the focussing and defocussing effects of turbulence. Below the first harmonic peak, in both Figure 8 and Figure 9, the first large ground dip occurs at approximately 60 Hz and is well captured by both modeling approaches. The sound levels propagated from the Convair in this frequency range are too low to be measured and are largely masked by the ambient background noise. Below 40 Hz, the ambient background noise levels and the Convair sound propagated levels are comparable. It has to be noted that FFP calculations were only carried out at octave frequencies between 63 Hz and 500 Hz in the case of the 12000 ft flights.

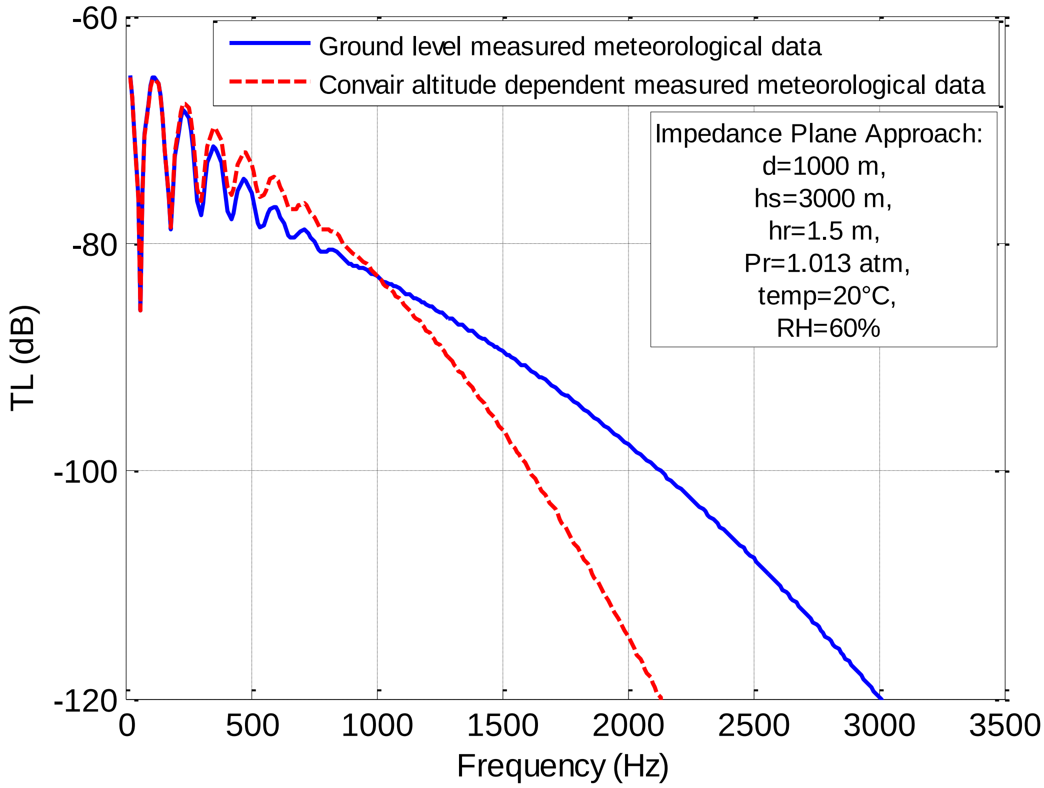


*Figure 5. Transmission Loss of acoustic propagation in atmosphere.*

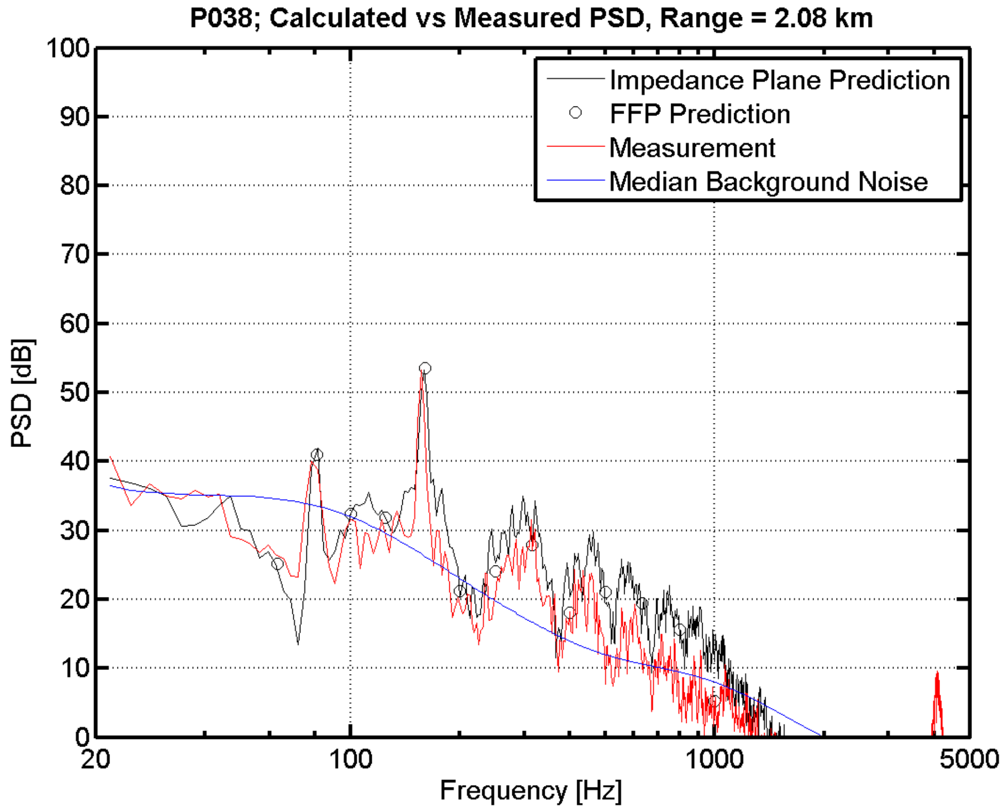


*Figure 6. Measured vs Predicted Spectra of Convair; Altitude 8000 ft, Range d = 2.08 km*

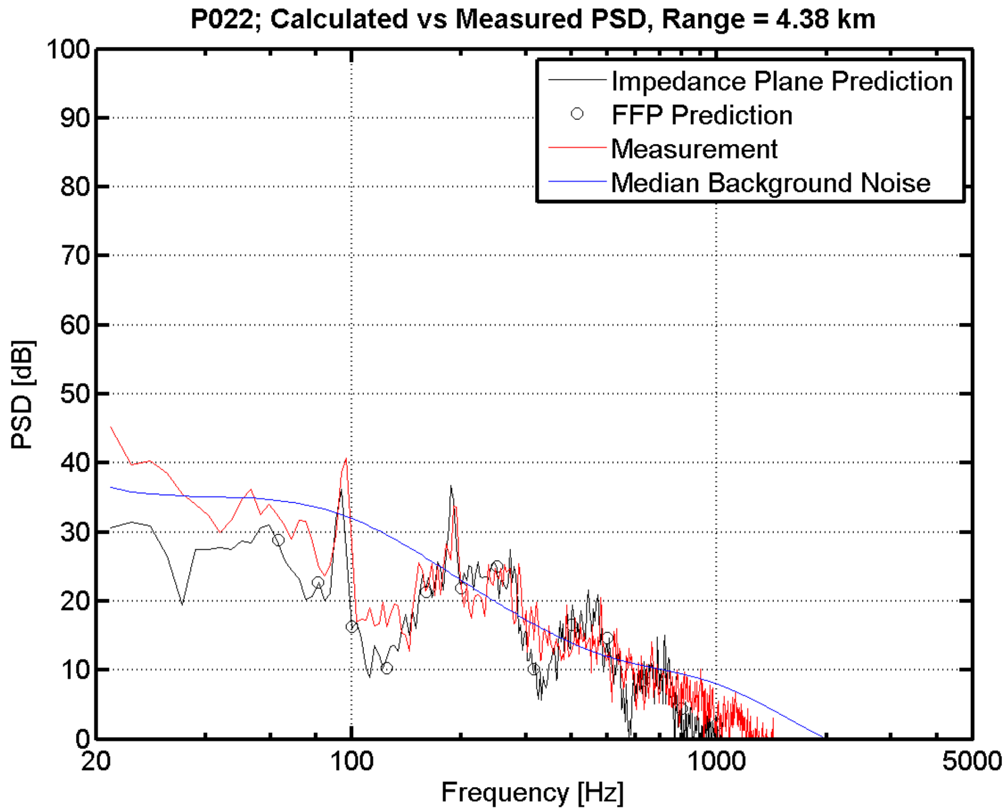


*Figure 7. Measured vs Predicted Spectra of Convair; Altitude 8000 ft, Range d = 4.38 km*

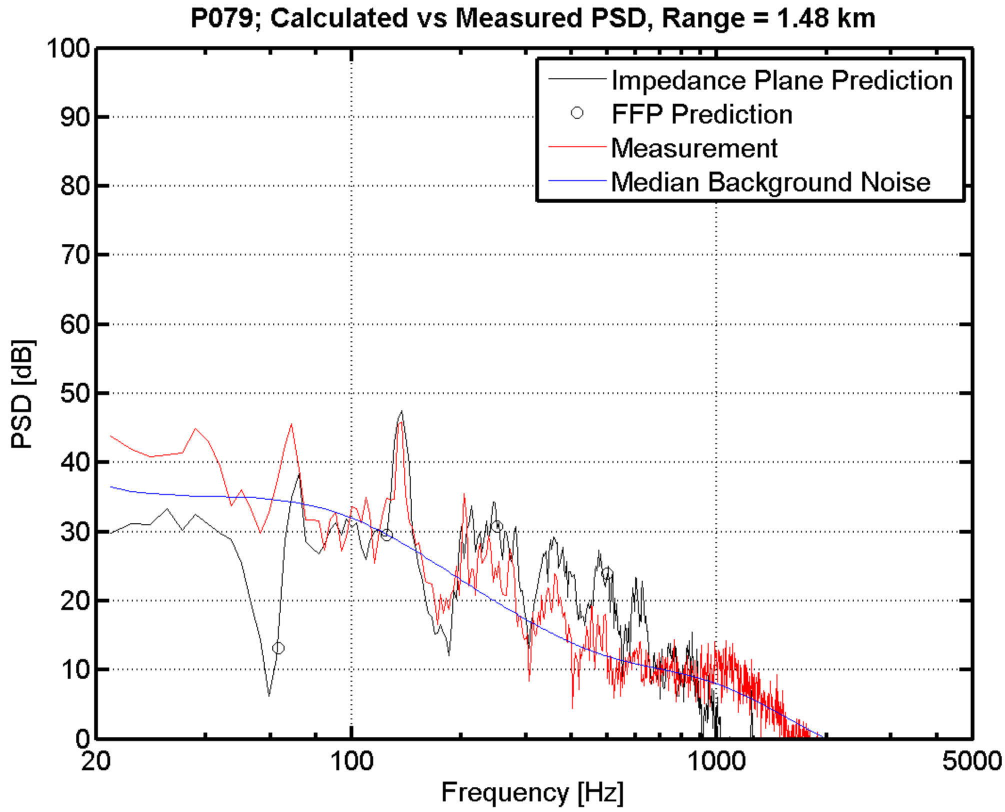


*Figure 8. Measured vs Predicted Spectra of Convair; Altitude 12000 ft, Range d = 1.48 km*

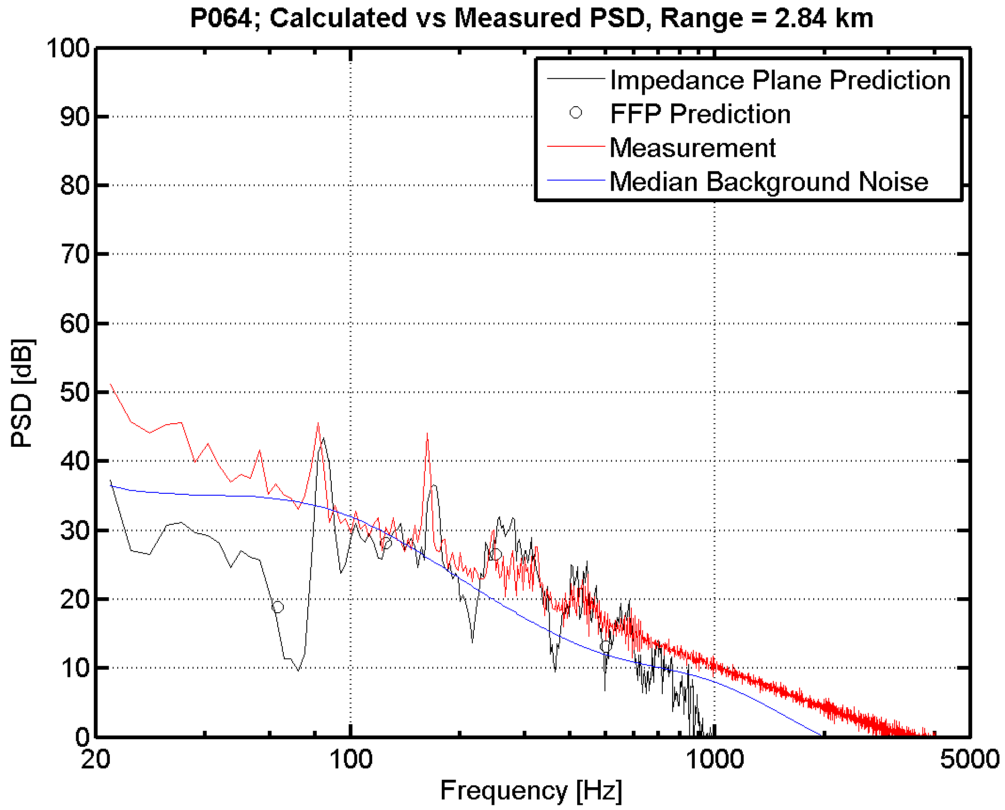


*Figure 9. Measured vs Predicted Spectra of Convair; Altitude 12000 ft, Range d = 2.84 km*

## 4. CONCLUSIONS

The impedance plane formulation and the Fast Field Program (FFP) were implemented to predict the acoustic spectra of an aircraft propagating through the atmosphere at various altitudes, distances and angles. The paper presented the numerical and testing validation results using the two theoretical approaches and discussed the influence of various factors on the aircraft sound propagation from high altitude. Moreover the good agreement between the two theoretical approaches considered demonstrated that that refraction is negligible. Additionally it has been demonstrated that meteorological measurements made only at ground level are insufficient to estimate the atmospheric absorption.

## 5. ACKNOWLEDGEMENTS

The authors would like to acknowledge the support of their colleagues at the Flight Research Laboratory: Anthony Brown, Peter Earle, Paul Kissmann, Robert Erdos, Mengistu Wolde, Derek Gowanlock, Konstantin Baibakov and Cuong Nguyen.

## 6. REFERENCES

**1.** L.C. Sutherland and G.A. Daigle, "Atmospheric Sound Propagation," in Encyclopaedia of Acoustics, Malcolm J. Crocker, Ed.: John Wiley and Sons, 1997, Chapter 32.

**2.** K. Attenborough et al., "Benchmark cases for outdoor sound propagation," Journal of the Acoustic Society of America, vol. 97, pp. 173-191, 1995.

**3.** E.M. Salomons, Computational Atmospheric Acoustics, Kluwer Academic Publishers, 2001.

**4.** G. A. Daigle, "Effects of atmospheric turbulence on the interference of sound waves above a finite impedance boundary," Journal of the Acoustic Society of America, vol. 65, pp. 45-49, 1979.

**5.** G. A. Daigle, J. E. Piercy, and T. F. W. Embleton, "Effects of atmospheric turbulence on the interference of sound waves near a hard boundary," Journal of the Acoustic Society of America, vol. 64, pp. 622-630, 1978.

**6.** S. Ghinet, A. Price, G. Daigle, M. Stinson, A. Grewal, and V. Wickramasinghe, "Atmospheric Propagation Model Validation with the NRC Convair 580 Aircraft," INTER-NOISE Congress and Conference Proceedings, InterNoise18, Chicago, USA.

**7.** A Price, S. Ghinet, A. Grewal, U. Yapa, V. Wickramasinghe, G. Daigle, M. Stinson, C. Minwalla, "Acoustic Atmospheric Propagation Model Validation with the NRC Convair 580," AIAA Scitech 2019 Forum, 2019, San Diego, California, USA.

**8.** H. E. Bass, L. C. Sutherland, A. J. Zuckerwar, D. T. Blackstock, and D. M. Hester, "Atmospheric absorption of sound: Further developments," Journal of the Acoustical Society of America 97, pp. 680-683, 1995.

**9.** Delany M. E. and Bazley E. N., Acoustical properties of fibrous absorbent materials, Applied Acoustics 3pp. 105-116, 1970,.

**10.** T. F. W. Embleton, J. E. Piercy, and G. A. Daigle, "Effective flow resistivity of ground surfaces determined by acoustical measurements," Journal of the Acoustical Society of America 74, pp. 1239-1244, 1983.

**11.** R. Raspet, and W. Wu, "Calculation of average turbulence effects on sound propagation based on the fast field program formulation," Journal of the Acoustical Society of America, Vol. 97, pp. 147-153, 1995.

**12.** Attenborough K, Hayek S and Lawther J, "Propagation of sound above a porous half-space," Journal of the Acoustical Society of America, Vol. 68, Issue 5, 1493–1501, 1980.

**13.** Brian Jamison, Mark Govett, Stan Benjamin, Kevin Brundage, and John M. Brown, Generate soundings from Rapid Refresh (RAP), FIM, GFS, NAM, and other Model Analyses and Forecasts, RAOBS, or Aircraft (restricted). [Online]. https://rucsoundings.noaa.gov/., Version: 3-Oct-2018.